

OPTIMIZATION OF MEASUREMENTS IN THE GEODETIC NETWORK FOR MONITORING THE HORIZONTAL DEFORMATIONS OF THE ROGOJEȘTI DAM

Constantin CHIRILĂ, Associate Professor, Ph.D Eng., Technical University „Gheorghe Asachi” of Iasi, Faculty of Hydrotechnical Engineering, Geodesy and Environmental Engineering, Department of Land Surveying and Cadastre, Romania, constantin.chirila@tuiasi.ro

Bianca Paula SIMINICARU – Master Eng., Technical University „Gheorghe Asachi” of Iasi, Faculty of Hydrotechnical Engineering, Geodesy and Environmental Engineering, Romania, siminicarubianca@yahoo.com

Cristian CUCOARĂ – Eng., S.C. CAR TOP S.R.L., Romania, office@cartop.ro

Abstract: *The monitoring of the horizontal deformations of the dams in Romania was done by means of classical geodetic methods of angular measurements and, sometimes, of distance measurements. With the advent of GNSS technology, testing the capability of spatial geodetic networks to meet the precision requirements in monitoring the horizontal deformations of the engineering structures has begun. The case study was carried out for the monitoring network of the Rogojești dam, which is made of local materials and located on the Siret River, 12 km from its entrance in the north of Romania. Optimization of measurements in the monitoring network has been analysed from the perspective of global precision indicators (standard reference deviation) and errors in the horizontal positioning of new points, highlighted by the graphical representation of standard error ellipses. The optimization problems were taken into consideration by both the classic geodetic micro-triangulation network and the modern GNSS network, used either individually or through the horizontal distance components, in a combined micro-triangulation-trilateration geodetic network. The conclusions highlight that by combining both classical measurements (angular measurements) and GNSS measurements (by horizontal distance determinations), positioning errors can be diminished and an improvement in the geometric configuration of the error ellipses in the newly determined points compared to the simple network of geodetic micro-triangulation becomes noticeable.*

Keywords: *deformations, monitoring, dam, network, optimization.*

1. Introduction

The Rogojești water storage on the Siret River (*figure 1*) is 12 km from its entrance to the country, at the communes of Mihăileni (left bank) and Grămești (right bank). Among the reservoir functions are the regularization of flows in the Siret Superior river basin, supplementing flows for drinking and industrial water supply in the Botoșani - Dorohoi area, transit of a sanitary flow on the Siret River, flood protection, supplementing deficit irrigation and producing electricity.

The storage lake has a length of 10 km and an area of 8 km², and in order to achieve the net storage volume and to avoid the permanent flooding of some agricultural land surfaces, defensive dikes with a length of about 3 km were provided in the tail of the lake on both shores.



Figure 1 - The location of the Rogojești water storage (@ Google Map)

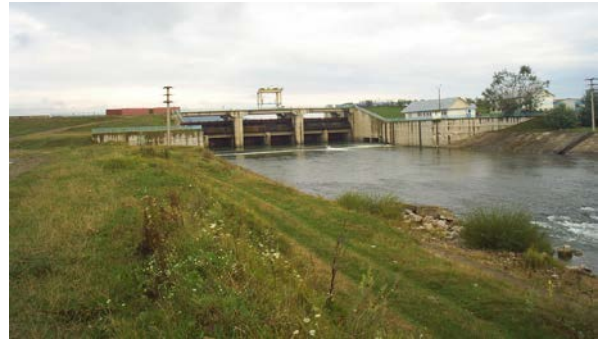


Figure 2 - The Rogojești Dam

The accumulation dam is a mixed dam, made up of several parts (figure 2). The front dam is a concrete dam type evacuator, with a length of 72 m, a width of 70 m and a maximum height of 23 m. The side dams are made of local materials (earth) with lengths of 2.2 km (left bank) and 1.2 km (right bank) and a maximum height of 14 m.

The geodetic equipment is composed of 8 cylindrical concrete pillars (P1...P8) and 14 target points, all with standard centring bolts (figure 3).

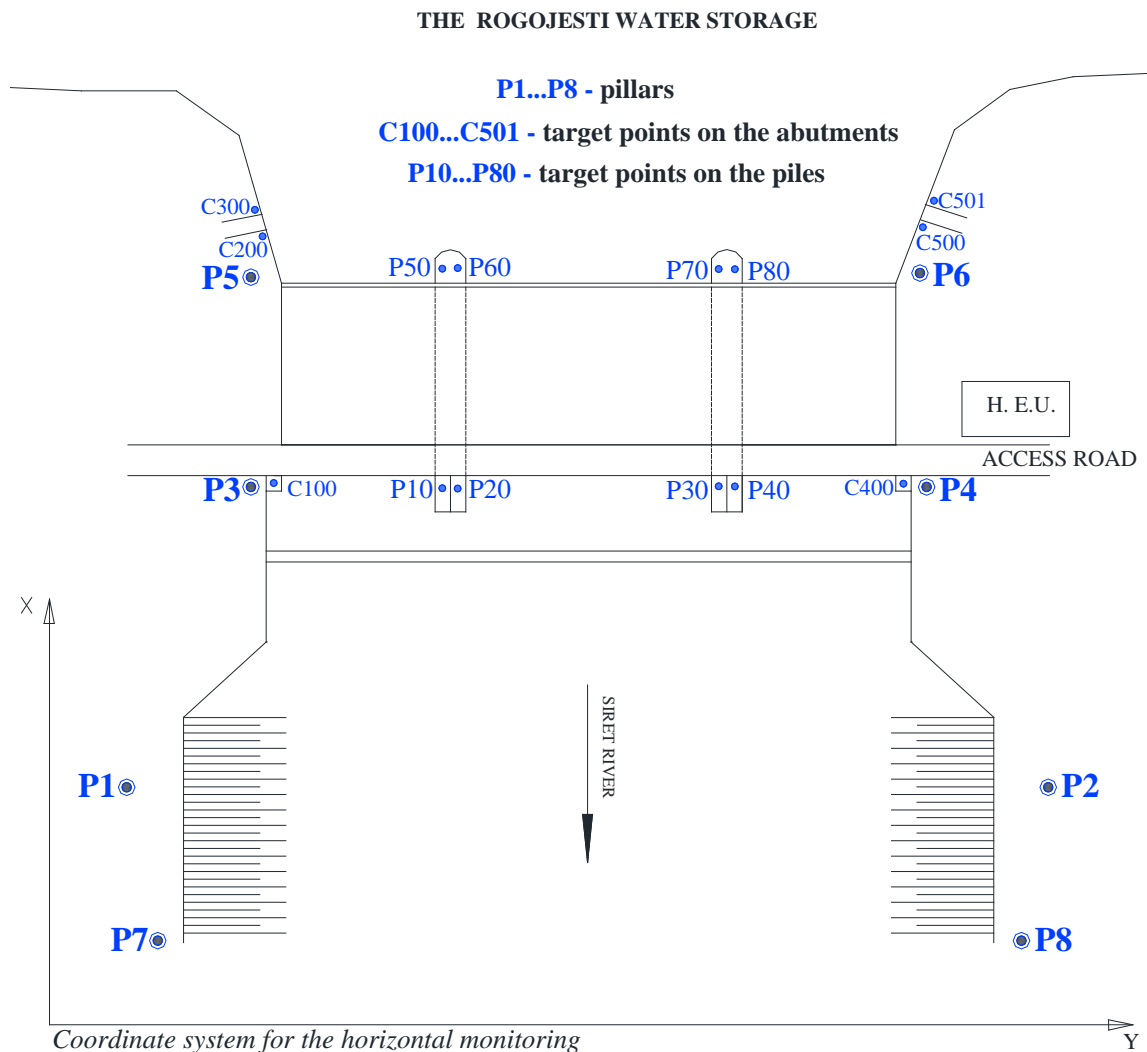


Figure 3 –Layout of geodetic equipment for the horizontal monitoring of the Rogojești dam

2. Study of the geodetic micro-triangulation network

The triangulation measurements in the current series were performed with a Topcon IS 201 total station, according to the visa sketch in *figure 4*, having P1 and P2 as control points.

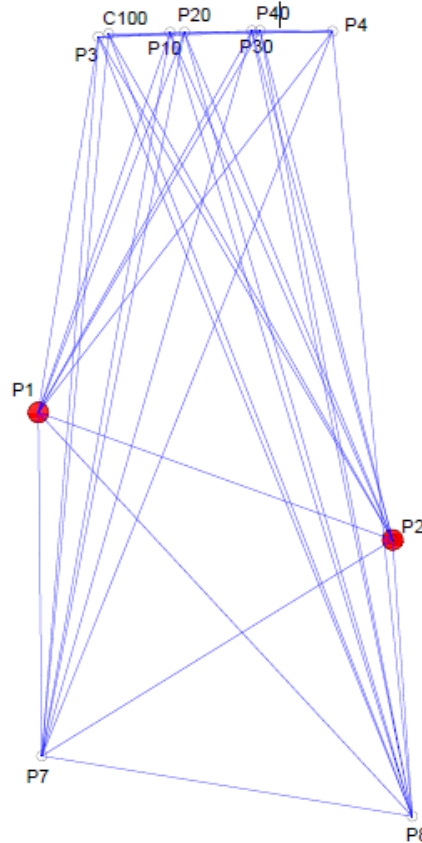


Figure 4 - The measuring directions in the geodetic micro-triangulation network

The error analysis after adjustment for several types of network processing was performed with „Adjust 7.0” free educational software.

In a first stage, only the pillars network was considered, which was adjusted as a minimum constrained network on the fixed points P1 and P2. The new points were represented by the pillars P3, P4, P7 and P8.

Estimated angle measurement errors were calculated with the formula $1''\sqrt{2} \approx 4.4''$, corresponding to the angular accuracy of the total station measurement (1").

The adjusted coordinates and the estimated standard deviations for determining the new points are presented in *table 1*, and based on them the error ellipses were represented graphically in *figure 5*.

Table 1 – Minimum constrained adjustment of the micro-triangulation pillars network

Point	The plane coordinates		The estimated standard deviations		The semiaxes of the error ellipse		The orientation of the ellipse
	X (m)	Y (m)	Sx (mm)	Sy (mm)	A (mm)	B (mm)	θ_A (°)
P3	1111.095	517.722	3.4	1.9	3.6	1.5	19.76
P4	1112.746	586.873	2.9	3.9	4.2	2.4	63.05
P7	898.420	501.042	2.1	2.2	2.2	2.1	124.21
P8	880.533	610.443	3.1	1.3	3.1	1.2	176.08

In order to test the “*all included*” adjustment, in which the mobile points P10 ÷ P40 are added to the new points, several variants were performed, because in the first adjustment two angles with possible blunders were highlighted and the χ^2 test at 95.0% significance level failed to pass. In the second adjustment the two angles were not eliminated, as this would have led to a maximum error of 8.7 mm at point P10, but the weights of the two angular observations were changed by increasing the estimated errors ($\approx 40^{\text{cc}}$). Thus, no possible blunders are reported after processing, the maximum error in horizontal position decreases to 5.7 mm at point P10, but the χ^2 test failed to pass. In the third “*all included*” adjustment variant, the weights were changed in the case of five angles whose standardized residuals were identified as high value, the final result being acceptance of the χ^2 test and the decrease of the maximum error to 3.6 mm at point P4.

For the constrained adjustment of the mobile points network at the fixed points represented by the previously adjusted pillars, the input data from the last “*all included*” adjustment were maintained, in which the weights statistically corresponded to the measured angles. The processing results reveal that there are no blunders and the χ^2 test is passed. The maximum error is observed in points P30 and P40, amounting to 2.2 mm (Table 2). Also, the configuration of the error ellipses for the target points P10 ÷ P40, can be seen in figure 6.

Table 2 – Full constrained adjustment of the micro-triangulation network

Point	The plane coordinates		The estimated standard deviations		The semiaxes of the error ellipse		The orientation of the ellipse
	X (m)	Y (m)	Sx (mm)	Sy (mm)	A (mm)	B (mm)	θ_A (°)
P10	1112.356	538.932	1.3	1.8	1.8	1.2	81.33
P20	1112.435	543.139	0.9	1.8	1.8	0.9	88.21
P30	1112.847	563.096	0.8	2.2	2.2	0.8	87.97
P40	1112.925	565.508	0.4	2.2	2.2	0.4	89.71

The statistical results of all adjustment variants, extracted from the final processing report, are presented in Table 3.

Table 3 – Statistical results of micro-triangulation network adjustment

Network type	Adjustment type	No. iterations	Redundancy	Reference standard deviation So	χ^2 lower value	χ^2 upper value	χ^2 test 95.0%	Data snooping method
Pillars	Minimum constrained	2	13	± 0.9	5.01	24.74	passed	without blunder detection
Pillars + target points	Minimum constrained	2	27	± 2.1	14.57	43.19	failed to pass	P4-P3-P10; P8-P3-P10 angles
Pillars + target points	Minimum constrained	2	27	± 1.4	14.57	43.19	failed to pass	without blunder detection
Pillars + target points	Minimum constrained	2	27	± 1.1	14.57	43.19	passed	without blunder detection
Pillars + target points	Full constrained	2	35	± 1.2	20.57	53.20	passed	without blunder detection

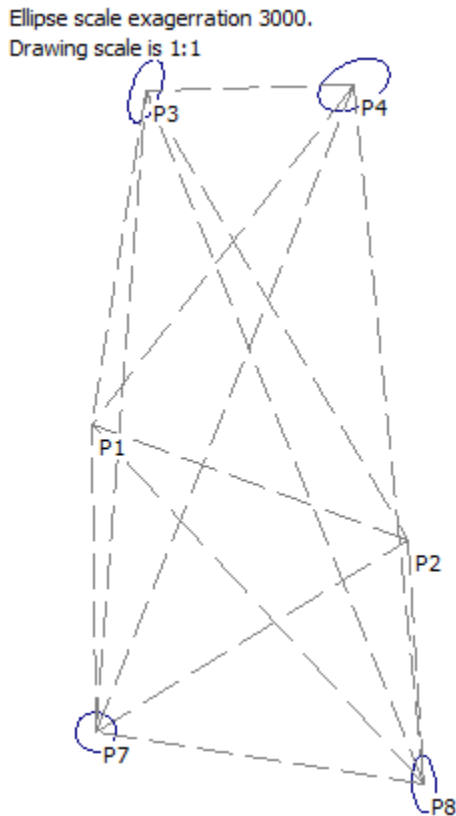


Figure 5 - Micro-triangulation network: error ellipses for the minimum constrained network

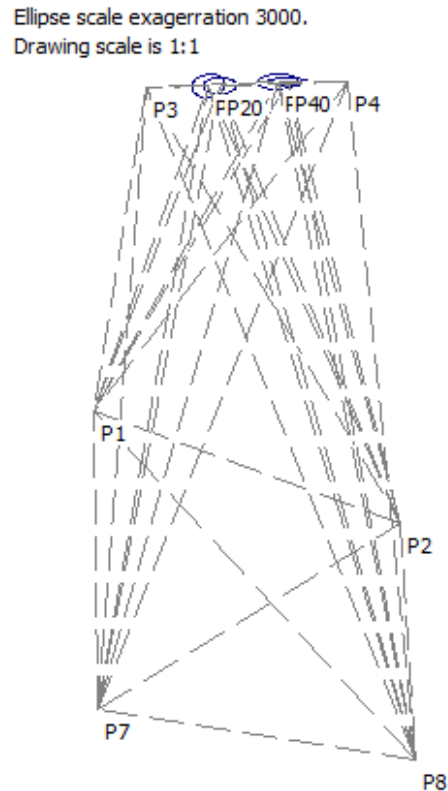


Figure 6 - Micro-triangulation network: error ellipses for the full constrained network

3. Study of the GNSS monitoring network

The GNSS monitoring network was designed on the old classic network in a local coordinate reference system, based on the WGS84 ellipsoid and a double stereographic projection (tangent plane) with natural origin at point P1 ($B = 47^{\circ}55'44''.20352$, $L = 29^{\circ}09'00''.33343$) with false coordinates, X (North) = 1000 m, Y (East) = 500 m. The orientation of the network is considered on the direction of pillars P1 - P2.

Eight GNSS receivers (TOPCON GR5, TOPCON HIPER PRO, SOKKIA GRS 270 ISX) were used to perform the measurements by the static method, using observation sessions from 40 minutes (in point P3) to 6 hours and 30 minutes (in point P1).

The processing of GNSS vectors was done automatically in the Leica Geo Office software, by including 17 stations and 72 GNSS vectors (*figure 7*).

The free network adjustment allowed the check of the internal geometry of the network and the possible blunder detection in the measurement data. The horizontal positioning components have estimated standard deviations that were up to 1.8 mm in the East (Y) direction and 2.7 mm in the North (X) direction, respectively, so with a horizontal positioning precision of up to 3.1 mm (*figure 8*).

In the case of adjusting only the pillars network (the mobile points will be determined from the constrained pillars network), the results obtained do not differ significantly, the differences on coordinates of the points in the constrained and in the free network being submillimetric.

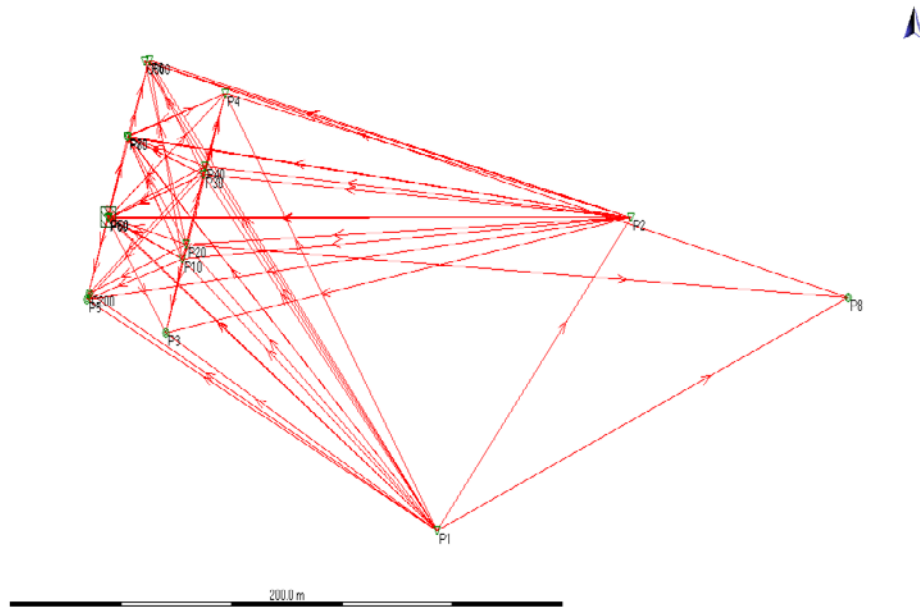


Figure 7 - GNSS vectors of the monitoring network

Point Id	Point Class	Date/Time	Easting	Northing	Ellip. Hgt.	Sd. Easting	Sd. Northing	Sd. Height	Posn. Qty	Hgt. Qty	Posn. + Hgt. Qty
<input checked="" type="checkbox"/> C200	Adjusted	01/12/2018 13:48:51	373.9528	1063.8049	336.4591	0.0011	0.0026	0.0088	0.0028	0.0088	0.0092
<input checked="" type="checkbox"/> C500	Adjusted	01/12/2018 13:48:51	394.0497	1126.8004	336.5059	0.0012	0.0020	0.0109	0.0023	0.0109	0.0111
<input checked="" type="checkbox"/> P1	Adjusted	01/12/2018 13:48:51	499.7716	999.2017	329.4851	0.0003	0.0004	0.0022	0.0005	0.0022	0.0023
<input checked="" type="checkbox"/> P10	Adjusted	01/12/2018 13:48:51	407.6921	1073.1875	336.5703	0.0005	0.0007	0.0043	0.0009	0.0043	0.0044
<input checked="" type="checkbox"/> P2	Adjusted	01/12/2018 13:48:51	570.0051	1084.4850	330.1887	0.0003	0.0004	0.0024	0.0005	0.0024	0.0024
<input checked="" type="checkbox"/> P20	Adjusted	01/12/2018 13:48:51	409.0229	1077.1361	336.5694	0.0004	0.0006	0.0036	0.0008	0.0036	0.0037
<input checked="" type="checkbox"/> P3	Adjusted	01/12/2018 13:48:51	401.7768	1052.9281	337.8401	0.0014	0.0019	0.0109	0.0024	0.0109	0.0111
<input checked="" type="checkbox"/> P30	Adjusted	01/12/2018 13:48:51	415.3052	1095.9496	336.6085	0.0004	0.0006	0.0036	0.0007	0.0036	0.0037
<input checked="" type="checkbox"/> P4	Adjusted	01/12/2018 13:48:51	423.3516	1118.1651	337.9309	0.0009	0.0014	0.0069	0.0017	0.0069	0.0071
<input checked="" type="checkbox"/> P40	Adjusted	01/12/2018 13:48:51	416.0446	1098.2233	336.6045	0.0005	0.0008	0.0044	0.0009	0.0044	0.0045
<input checked="" type="checkbox"/> P5	Adjusted	01/12/2018 13:48:51	373.0984	1062.1821	337.5367	0.0010	0.0011	0.0077	0.0015	0.0077	0.0078
<input checked="" type="checkbox"/> P50	Adjusted	01/12/2018 13:48:51	381.0393	1084.4748	336.5118	0.0005	0.0010	0.0051	0.0011	0.0051	0.0052
<input checked="" type="checkbox"/> P6	Adjusted	01/12/2018 13:48:51	395.8173	1127.1622	337.5870	0.0018	0.0021	0.0149	0.0028	0.0149	0.0152
<input checked="" type="checkbox"/> P60	Adjusted	01/12/2018 13:48:51	380.9289	1084.0991	336.5493	0.0004	0.0006	0.0034	0.0007	0.0034	0.0034
<input checked="" type="checkbox"/> P70	Adjusted	01/12/2018 13:48:51	388.0773	1106.3111	336.5633	0.0006	0.0010	0.0054	0.0012	0.0054	0.0055
<input checked="" type="checkbox"/> P8	Adjusted	01/12/2018 13:48:51	648.4566	1062.5702	329.9280	0.0016	0.0027	0.0120	0.0031	0.0120	0.0124
<input checked="" type="checkbox"/> P80	Adjusted	01/12/2018 13:48:51	388.0160	1106.1750	336.5724	0.0008	0.0009	0.0097	0.0012	0.0097	0.0098

Figure 8 – The results of the free network adjustment in the Leica Geo Office software

In order to ensure the connection between the coordinates obtained in the GNSS processing (*system 1*) with the local coordinate reference system of the monitoring network from the previous cycles (*system 2*), the 2D Helmert transformation was performed, having the P1 and P2 pillars as common points. In this case, the horizontal network adjusted in the current cycle as a free network, will be minimally constrained on the two chosen points by a translation, rotation and scaling operation:

$$\begin{pmatrix} x \\ y \end{pmatrix}_{sistem_2} = \begin{pmatrix} \Delta x \\ \Delta y \end{pmatrix}_{1 \rightarrow 2} + \begin{pmatrix} a & -b \\ b & a \end{pmatrix} \begin{pmatrix} x \\ y \end{pmatrix}_{sistem_1}$$

where $(\Delta x, \Delta y)$ are the translation constants and the parameters (a, b) include the scale factor (k) and the rotation angle (α) : $a = k \cos \alpha$; $b = k \sin \alpha$ (table 4).

Table 4 – 2D transformation parameters and transformed plane coordinates of the pillars

2D transformation parameters	Value	New points	Transformed plane coordinates	
			X (m)	Y (m)
Δx	-616.497 m	P3	1111.095	517.717
Δy	1135.115 m	P4	1112.752	586.866
a	0.3388835	P5	1141.415	516.771
b	-0.9478894	P6	1141.901	586.064
a (rotation)	289°40'21".6	P8	880.537	610.453
k (scale factor)	1.00665			

4. Optimization of the horizontal monitoring network

Comparing the 2D/GNSS monitoring network and the minimum constrained micro-triangulation network, a maximum difference of 4.8 mm on the X axis and 10.9 mm on the Y axis results for common pillars, hence a maximum horizontal positioning difference of 11.9 mm (in point P8).

Assuming the establishment of the same initial conditions in both micro-triangulation and GNSS networks, a first verification consists in comparing the values of the distance between the basic pillars P1 and P2, obtained from the known coordinates and from the GNSS determinations, respectively:

$$D_{P1-P2}^* = \sqrt{\Delta X_{P1-P2}^2 + \Delta Y_{P1-P2}^2} = 111.215 \text{ m}; \quad D_{P1-P2}^o = 111.488 \text{ m}.$$

The difference between the calculated and measured distance values ($D^* - D^o$) is 0.734 m, which leads to the conclusion that the approach of a constrained adjustment (including both directions and distances) would lead to results affected by blunders. This is due to the fact that the use of known coordinates of the control points in the micro-triangulation network results in a network scaling error, which makes it inappropriate to use them as constraints for accurate determinations of distances resulting from the measurement of GNSS bases.

In this case, the full adjustment of all angular and distance measurements will be performed based on the plane coordinates of the local reference system defined in the GNSS project. During the GNSS measurements it was not possible to use P7 pillar as a station, but the plane coordinates of this point are needed in the adjustment of the micro-triangulation-trilateration network. These could be determined by the back intersection procedure, using angular measurements from the micro-triangulation network.

Depending on the local precision and the configuration of the error ellipses in the newly determined points, to be obtained from the adjustment of the monitoring network, it was agreed to select horizontal distances from GNSS measurements, which will enter into rigorous processing with angular micro-triangulation measurements. The horizontal distances resulting from the measured GNSS bases also have the advantage of supporting those directions that have no visibility. By unified processing of both azimuthal directions and horizontal distances, an adjustment of a micro-triangulation-trilateration network results, using the least squares method by indirect observations.

The ellipsoidal distances from the GNSS measurements were obtained within the WolfPack software, where inverse geodetic problem solving function is called, for which it is necessary to know the geodetic coordinates of the two end points of the GNSS vector. These values are extracted from the reports obtained in the Leica Geo Office software.

As the map projection was defined as a double stereographic projection with the plane tangent to the point P1 of the monitoring network and given the small distances between the points of the network (of the order of hundreds of meters), it can be considered that the horizontal distances will be identical to those on the ellipsoid, due to small (submillimeter) corrections, resulting from the reduction of the distances from the ellipsoid in the projection plane.

Next, the same adjustment variants that have been applied in the micro-triangulation network will be presented, respectively as a minimum constrained and then full constrained network, with all the steps to improve the precision of determining the position of the new points. It is noted that in the case of micro-triangulation-trilateration networks, the degrees of freedom are 3, which for the horizontal monitoring network means the plane coordinates of the pillar P1 (x,y) and the reference orientation (θ) of the direction pillars P1 - P2.

As a minimum constrained network, only the network of common pillars with those from the micro-triangulation network was initially considered, and then it was extended to all existing pillars, and finally, also to the mobile points. The estimated errors of the measured distances were calculated in relation to the estimated standard deviations of the spatial distances determined in the processing of the GNSS bases.

The adjusted coordinates for the new points and their estimated standard deviations in the pillar network are presented in *Table 5*.

Table 5 – Minimum constrained adjustment of the triangulation-trilateration pillars network

Point	The plane coordinates		The estimated standard deviations		The semiaxes of the error ellipse		The orientation of the ellipse
	X (m)	Y (m)	Sx (mm)	Sy (mm)	A (mm)	B (mm)	θ_A (°)
P2	1084.486	570.006	0.8	0.9	1.1	0.5	39.47
P3	1052.931	401.776	0.9	1.4	1.4	0.9	176.13
P4	1118.168	423.356	1.2	1.4	1.6	0.7	38.47
P7	966.206	595.142	1.5	1.7	1.9	1.2	36.10
P8	1062.561	648.460	1.2	1.6	1.7	0.9	150.31

Within the minimum constrained micro-triangulation - trilateration pillars network, it is noted that the major semi-axes of the error ellipses have values up to 1.9 mm, the χ^2 test is passed and there are no blunders in the measurement data.

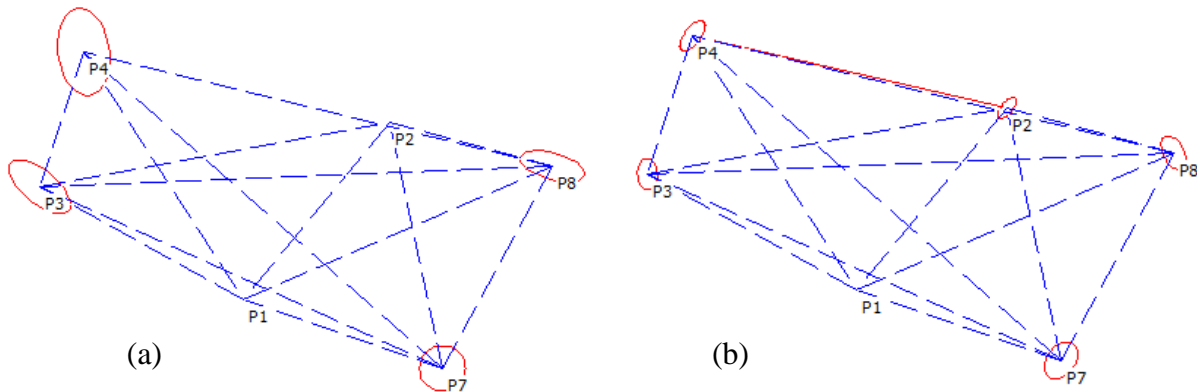


Figure 8 – Error ellipses within minimum constrained micro-triangulation network (a) and micro-triangulation-trilateration network (b)

Comparing the two networks, we notice that by introducing the distances there is an improvement of the values of the error ellipses semiaxes from the range 1.2 ÷ 3.6 mm to 0.5 ÷ 1.9 mm. The maximum difference between the plane coordinates of the pillars in the two types of network is 3.4 mm on the y-axis, at point P7.

Due to the fact that when introducing additional distances, regarding the P5 and P6 pillars, they can be determined (*Table 6*) together with the other ones (which was not possible in the triangulation measurements due to the lack of visibility between points and insufficient measurements), minimum constrained adjustment of the extended pillars network (*Figure 9*) and mobile points (*Figure 10.b*) was performed.

Table 6 – Minimum constrained adjustment of the extended pillars network

Point	The plane coordinates		The estimated standard deviations		The semiaxes of the error ellipse		The orientation of the ellipse
	X (m)	Y (m)	Sx (mm)	Sy (mm)	A (mm)	B (mm)	θ_A (°)
P5	1062.182	373.099	2.2	1.0	2.3	0.7	18.37
P6	1127.162	395.814	2.6	2.6	3.0	1.3	35.23

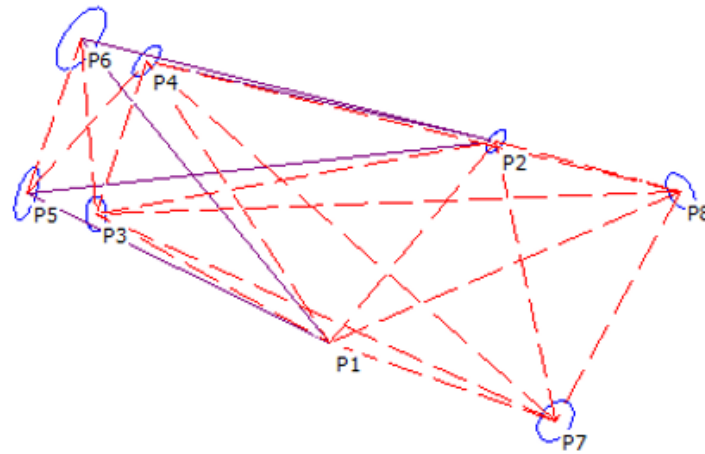


Figure 9 - Error ellipses within extended micro-triangulation-trilateration pillars network, related to minimum constrained processing

In the case of the extended pillars network, two adjustments were performed, the last being necessary to pass the χ^2 test, which led to the reduction of the major semiaxes of the error ellipses up to 2 mm, unlike the previous case (3 mm).

Comparing with the similar variant of adjustment of the micro-triangulation network, we observe the decrease of the major semiaxes from 3.5 mm to 1.9 mm and the improvement of the geometric configuration of the error ellipses in the target points (*Figure 10.b*). The error ellipses are arranged with the minor semiaxis on the transverse direction of the dam structure, where maximum deformations are expected due to the pushing force of the water. The maximum difference between the plane coordinates of the pillars and mobile points in the two types of network is 9.9 mm on the x-axis at point P40.

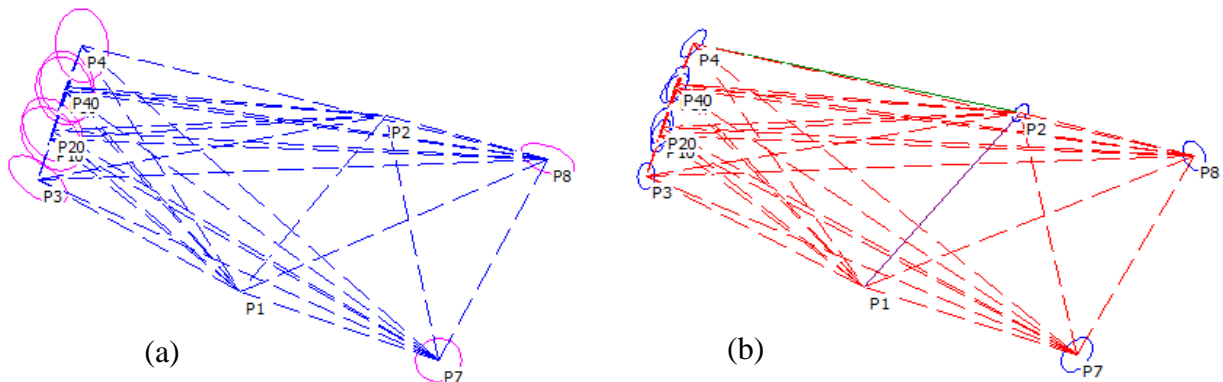


Figure 10 – Error ellipses within minimum constrained micro-triangulation network (a) and micro-triangulation-trilateration network (b)

Within the constrained network of micro-triangulation - trilateration, the pillars of the network are considered fixed points of known coordinates, and the target points on the dam structure (P10, P20, P30, P40) are the new points to be determined by adjustment. For this case only the first 6 pillars (P1, P2, P3, P4, P7, P8) were used to have a comparison similar to the case of the micro-triangulation network. Failure to pass the χ^2 test required a change in the measurement weights, so that the second adjustment variant was achieved with results presented in *table 7*. The major semiaxes of the error ellipses have values of up to 1.4 mm unlike the previous case (1.8 mm).

Table 7 – Full constrained adjustment of the micro-triangulation trilateration network

Point	The plane coordinates		The estimated standard deviations		The semiaxes of the error ellipse		The orientation of the ellipse
	X (m)	Y (m)	Sx (mm)	Sy (mm)	A (mm)	B (mm)	θ_A (°)
P10	1073.197	407.690	1.2	0.5	1.3	0.4	12.89
P20	1077.153	409.024	1.4	0.6	1.4	0.6	5.85
P30	1095.957	415.309	1.3	0.9	1.3	0.8	12.96
P40	1098.242	416.044	1.3	0.6	1.4	0.4	19.45

The constrained micro-triangulation-trilateration network was compared with a similar variant of the micro-triangulation network (*Figure 11*), with improved results in terms of reducing the maximum value of the major semiaxis of error ellipses from 2.2 to 1.4 mm.

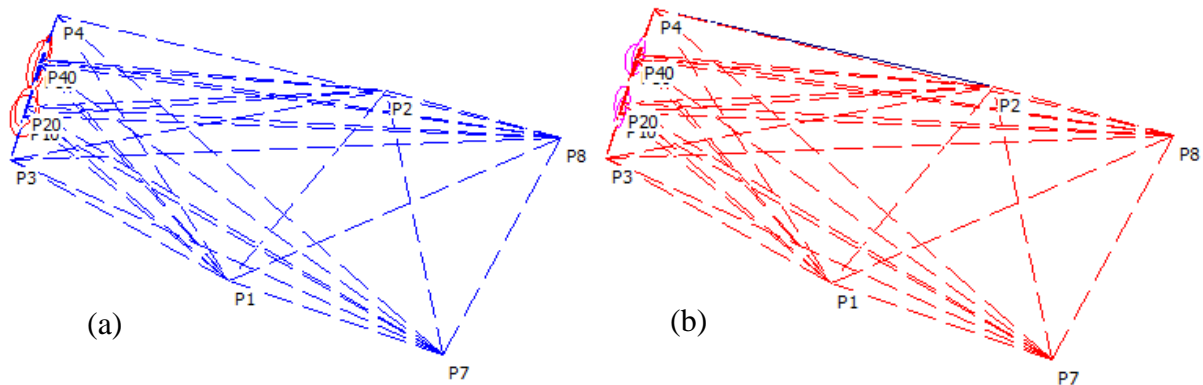


Figure 11 – Error ellipses within full constrained micro-triangulation network (a) and micro-triangulation-trilateration network (b)

The maximum difference between the plane coordinates of the mobile points in the two types of network is 4.5 mm on the X axis at point P30.

4. Conclusions

By comparing the distances between pillars P1 and P2 obtained from known coordinates and GNSS measurements, there is a significant difference, due to scaling error of the micro-triangulation network, which requires a reset of the measurement cycles.

If the beneficiary imposes angular measurements on the horizontal monitoring network, then it can improve its accuracy by adding horizontal distances derived from the GNSS vectors, some of which may complement the lack of visibility within the network.

We can conclude that by combining classic (angular) measurements and GNSS measurements (by determining horizontal distances), positioning errors are reduced and there is an improvement in the geometric configuration of error ellipses at the newly determined points, compared to the simple geodetic micro-triangulation network.

5. References

1. Chirilă C., - *Mathematical geodesy. Practical works and project. Tehnopress Publishing House, Iasi, 2014.*
2. Ghilani D.C., Wolf P.R., - *Elementary Surveying. An introduction to Geomatics. 13th Edition, Pearson Education, Inc., Upper Saddle River, New Jersey, U.S.A., 2012.*
3. Ghilani D.C., Wolf P.R., - *Adjustment computations. Spatial data analysis. Fourth edition, John Wiley & Sons, Inc, Hoboken, New Jersey, S.U.A., 2006.*
4. Nistor Gh. – *Applied geodesy for constructions study, „Gh. Asachi” Publishing House, Iasi, 1993.*
5. *** <http://www.personal.psu.edu/cdg3/free.htm>